Side Stream Control in Semicontinuous Distillation

Authors:

Pranav Bhaswanth Madabhushi, Thomas Adams II

Date Submitted: 2018-10-18

Keywords: Semicontinuous Distillation, side stream control, dynamical system analysis, dynamic optimization

Abstract:

The idea to reduce cycle time (?), by controlling the side stream flow rate using a feedforward control model -- the ideal side draw recovery arrangement (ISR) -- was standard in most semicontinuous distillation studies. However, its effect, particularly on '?' and more broadly on the system dynamics, was not clearly understood. In the current study, we compare the performance of using a modified form of ISR model with the status quo, based on the criteria, ? and separating cost (SC) on different case studies. Results show that the modified control model performed better with a 10-20% reduction in SC while maintaining product purities. Furthermore, the side stream flow rate trajectory that minimizes SC was found by using dynamic optimization and it did not differ a lot from the trajectory generated by the modified control model. The improvement in SC was at most 2%.

Record Type: Preprint

Submitted To: LAPSE (Living Archive for Process Systems Engineering)

Citation (overall record, always the latest version):	LAPSE:2018.0738
Citation (this specific file, latest version):	LAPSE:2018.0738-1
Citation (this specific file, this version):	LAPSE:2018.0738-1v1

DOI of Published Version: https://doi.org/https%3A//doi.org/10.1016/j.compchemeng.2018.09.002

Side Stream Control in Semicontinuous Distillation

Pranav Bhaswanth Madabhushi[a], Thomas A. Adams II[a,*]

[a]*Department of Chemical Engineering McMaster University, 1280 Main St. West, Hamilton, Ontario, L8S 4L8, Canada.*

[*]*Corresponding author:* tadams@mcmaster.ca

Abstract

The idea to reduce cycle time (*T*), by controlling the side stream flow rate using a feedforward control model -- the ideal side draw recovery arrangement (ISR) -- was standard in most semicontinuous distillation studies. However, its effect, particularly on '*T*' and more broadly on the system dynamics, was not clearly understood. In the current study, we compare the performance of using a modified form of ISR model with the status quo, based on the criteria, *T* and separating cost (SC) on different case studies. Results show that the modified control model performed better with a 10-20% reduction in SC while maintaining product purities. Furthermore, the side stream flow rate trajectory that minimizes SC was found by using dynamic optimization and it did not differ a lot from the trajectory generated by the modified control model. The improvement in SC was at most 2%.

Keywords: Semicontinuous distillation; side stream control; dynamical system analysis; dynamic optimization

1. Introduction

Distillation in process industries is a common separation technology with a major portion of plant operating costs associated with it (Adams and Pascall, 2012). Distillation systems are typically operated either in batches or continuously, where the choice is based on the production volume, feed composition, and product demand variability (Phimister and Seider, 2000a). Batch distillation is used in situations where the production demand is low or for high process flexibility, for example, pharmaceutical industries and biofuel production plants. Conversely, continuous distillation typically involves high volume production with low process flexibility—a common situation in petrochemical production facilities.

Alternatively, an atypical process for the separation of multicomponent mixtures is semicontinuous distillation. It is ideal for industries that are scaling up their production capacities from the batch mode, such as in pharmaceutical industries (Pascall and Adams, 2013).There are different categories of semicontinuous distillation, namely, zeotropic distillation, pressure-swing azeotropic distillation, extractive distillation, and semicontinuous distillation with integrated reaction (Adams and Pascall, 2012). In this article, the focus is on the semicontinuous distillation of multicomponent zeotropic mixtures, hereafter referred to as just semicontinuous distillation. Semicontinuous distillation is carried out using middle vessels (MVs) tightly integrated with a

distillation column through side stream recycle. This process was demonstrated to have a lower capital investment when compared to an equivalent continuous distillation process for intermediate production ranges in many different case studies (Meidanshahi and Adams, 2015; Pascall and Adams, 2014, 2013, Wijesekera and Adams, 2015a, 2015b). Unlike the continuous counterpart that ideally operates at a steady state, semicontinuous distillation is a forced periodic process, which is described next.

1.1 Semicontinuous distillation: Process

To separate a ternary zeotropic mixture of *A, B,* and *C* semicontinuously, one MV and one distillation column are required (Phimister and Seider, 2000a). Semicontinuous distillation entails periodic repetition of the three modes of operation, namely, the Charging (*Ch*), the Separating (*Sep*) and the Discharging (*Dis*) modes (Adams and Pascall, 2012). Figure 1 illustrates the mode transitions in a semicontinuous process. The mode transitions occur when the mole fraction of component B in the MV ($x_{MV,B}(t)$) and/or height of liquid in the MV ($h_{MV}(t)$) (system states) periodically reach some pre-defined values during operation. The times at which the modes begin (or end) is dependent on these states and is not known *a priori*.

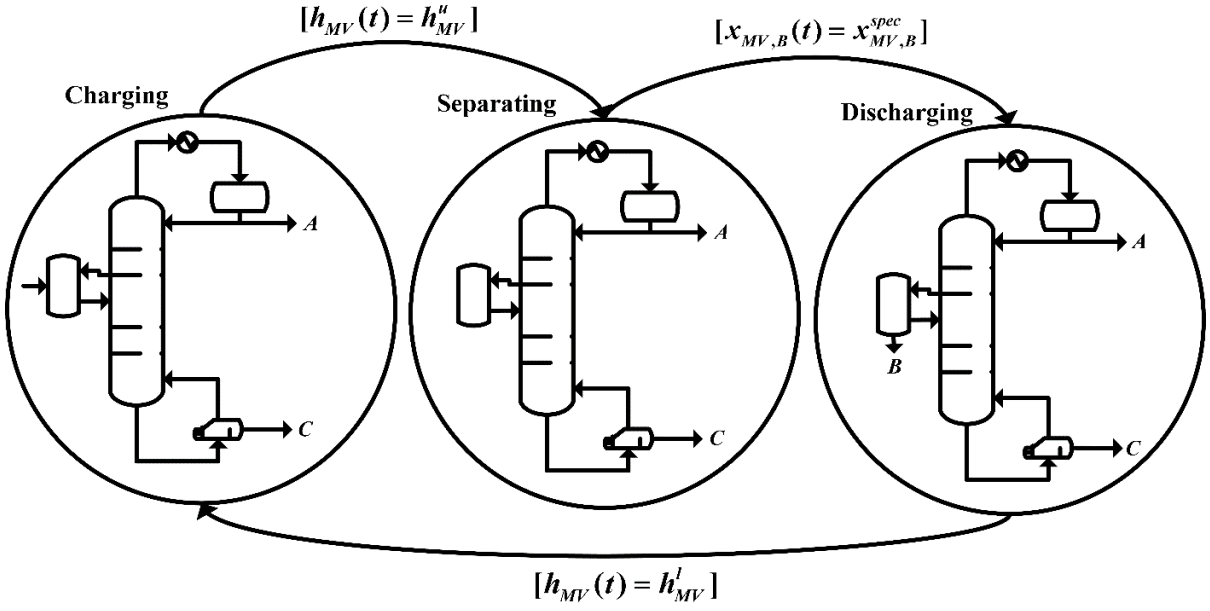

Figure 1: State diagram illustrating modes and mode transitions during a semicontinuous distillation process

In a representative semicontinuous cycle, the MV continuously feeds ($F(t)$) the distillation column, and a side stream ($S(t)$) from the column is continuously recycled to the MV during all modes. Furthermore, light (*A*) and heavy (*C*) components are continuously recovered from the distillate (*Di*) and bottoms (*Bo*) streams of the distillation column respectively at the desired purities,

although at decreasing flow rates as the cycle progresses. The MV has four material streams, two inlet streams and two outlet streams, and depending on the operating mode two or three streams are operational. The inlet streams supplying liquid to the MV are the side stream recycle $S(t)$ and the feed stream to the MV ($F_{MV}(t)$), and the two outlet streams drawing liquid from the MV are the column feed and the discharge stream ($F_{Dis}(t)$) (refer to Figure 2).

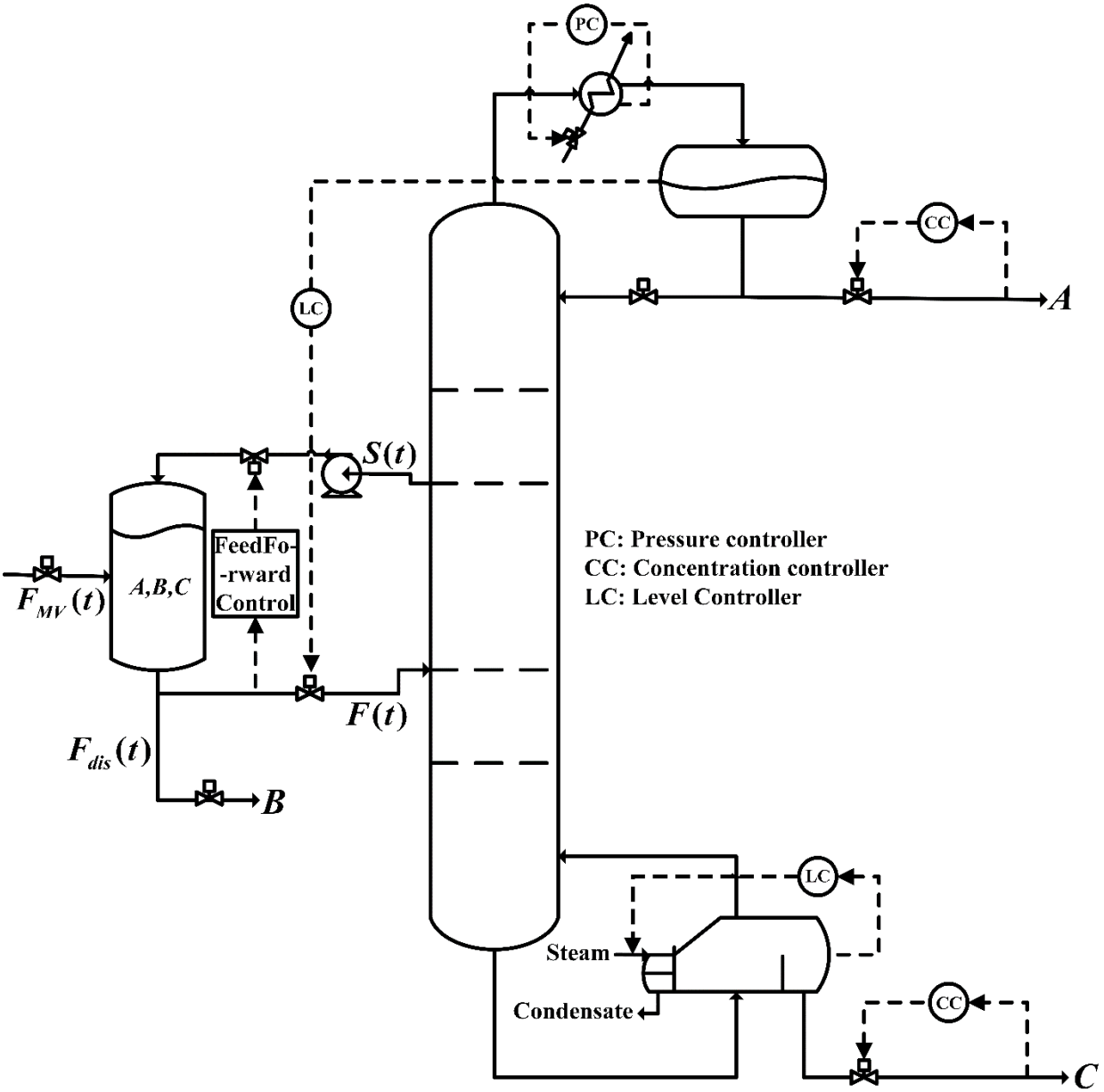

Figure 2: Control structure as suggested by Pascall and Adams, 2013. It uses DB control with reflux drum level controlled by manipulating $F(t)$, sump level controlled by manipulating the

reboiler duty ($Q_r(t)$), column pressure is controlled by manipulating condenser duty ($Q_c(t)$) and $S(t)$ is controlled using feedforward control.

In the separating mode, the MV has one functioning inlet stream, $S(t)$, and outlet stream, $F(t)$, while the other two streams are non-operational. A large fraction of the recovery of A and C components at the desired purities occurs during this mode. The side stream, which is higher in component B concentration than the contents of the MV, enriches the MV with this component as the mode advances to the end. When the mole fraction of component B in the MV ($x_{MV,B}(t)$) reaches the desired purity ($x^{spec}_{MV,B}$), the separating mode ends. Immediately, the discharging mode begins with the opening of the discharge valve of the MV ($v_{MV,Dis}(t)$) to collect component B at the desired purity. The discrete change in the input, $v_{MV,Dis}(t)$, has the following functional form:

$$v_{MV,Dis}\left(t,\, x_{MV,B}(t), h_{MV}(t)\right) \coloneqq\; v_{MV,Dis}(t) \;=\; \begin{cases} 0, & if\ charging\ or\ separating\ mode \\ 1, & if\ discharging\ mode \end{cases} \quad (1)$$

During the discharging mode, the MV has one functioning inlet stream, $S(t)$, and two functioning liquid streams, $F(t)$, and $F_{Dis}(t)$. The mode ends when $h_{MV}(t)$ falls below the pre-specified lower limit (h^{l}_{MV}). Instantaneously, the charging mode begins by fully opening the feed charging valve to the MV($v_{MV,Ch}(t)$) to charge fresh feed to be separated, and simultaneously fully closing the discharge valve. The discrete input that triggers this mode transition takes the functional form:

$$v_{MV,Ch}\left(t,\, h_{MV}(t)\right) \coloneqq\; v_{MV,Ch}(t) \;=\; \begin{cases} 0, & if\ discharging\ or\ separating\ mode \\ 1, & if\ charging\ mode \end{cases} \quad (2)$$

Finally, a mode transition between the charging and the separating mode is triggered by fully closing the charging valve when the height of liquid in the MV ($h_{MV}(t)$) reaches a pre-specified upper limit (h^{u}_{MV}). This is the beginning of the separating mode of a new cycle. The state dependent control inputs prevent the system from ever reaching a steady-state. The control system that drives this process is described next.

1.2 Semicontinuous Distillation: Control

The continuous side stream recycle introduces concentration dynamics in the MV, thus changing the column feed composition and consequently the distillate and bottoms product concentrations (mole fraction of component A in the distillate stream ($x_{Di,A}(t)$) and mole fraction of component C in the bottoms stream ($x_{Bo,C}(t)$ respectively) with time. Therefore, to maintain these product purities near the desired values during the cycle, the Distillate-Bottoms (DB) control configuration (illustrated in Figure 2) was proposed by Phimister and Seider (2000b). In this control configuration, the independent variables, $Di(t)$ and $Bo(t)$ are chosen for composition control from the available seven degrees of freedom, which are: (1) the distillate flow rate ($Di(t)$); (2) the bottoms flow rate ($Bo(t)$); (3) the reflux rate ($L(t)$); (4) the reboil rate ($V(t)$); (5) the feed flow rate to the column ($F(t)$); (6) the side stream flow rate ($S(t)$); (7) and the condenser duty ($Q_c(t)$). The

DB concentration control was shown to effectively handle off-spec products in semicontinuous distillation by Phimister and Seider (2000b), because the chosen manipulated variables are independent unlike the continuous counterpart.

In the seminal work on semicontinuous distillation by Phimister and Seider (2000a), the reflux drum level ($h_r(t)$) and the sump level ($h_s(t)$) were controlled using the reflux rate ($L(t)$) and the reboil rate ($V(t)$) respectively. These manipulated variables, which change the column internal flow rates directly affect the concentration profiles of the components within the column. The column pressure ($P(t)$) was controlled using $Q_c(t)$. However, significant details on the nature of $F(t)$ and $S(t)$ were not provided. Five degrees of freedom ($Di(t), Bo(t), L(t), V(t), Q_c(t)$) were used as manipulated variables to control the five outputs ($x_{Di,A}(t), x_{Bo,C}(t), h_r(t), h_s(t), P(t)$) near the desired values. Additionally, they also mathematically showed that the MV decouples the interactions in DB control configuration using the steady state relative gain method (Bristol, 1966).

Subsequently, an extensive control study conducted by Pascall and Adams (2013) evaluated the performance of several permutations of *DB* multi-loop control configurations in terms of set-point tracking and disturbance rejection. The authors concluded that the performance criteria were met successfully by controlling $h_r(t)$ using $F(t)$, $h_s(t)$ using the reboiler duty ($Q_R(t)$), *DB* concentration control and side stream control. Figure 2 illustrates this control structure, which will be referred to as the 'Pascall-Adams' control configuration in this study. The side stream, $S(t)$, is controlled using feedforward control with a control model called the Ideal Side draw Recovery (ISR) arrangement. The feedforward control was implemented via a feedback loop. One of the major limitations of the study conducted by Pascall and Adams (2013) was that the analysis did not cover the impact on the cycle time of the process when the control configuration is changed.

In an attempt to achieve better control performance for the semicontinuous distillation process, Meidanshahi et al. (2017) used cascaded subspace quality model predictive control (SQMPC). In this approach, the setpoints were given by the MPC – only during the separating mode – to all the controllers in the Pascall-Adams control configuration. The linear time invariant model for SQMPC was identified using the 'Subspace Model Identification' technique. The authors observed that the total cycle time (T) was reduced by 10% when compared with Pascall-Adams control configuration, but with $S(t)$ as a constant function. This study was the first known attempt in comparing the effect of changing the control philosophy on T and therefore on the Separating Cost (SC), which is defined as:

$$\mathrm{SC} = \frac{\frac{\text{Capital Cost}}{\text{3 Year Payback Period}} + \text{Annual Utility Cost}}{\text{Annual Amount of Purified Product Recovered}} \tag{3}$$

From their work, there is anecdotal evidence that $S(t)$ might have a significant impact on the SC.

In the present study, we attempt to understand how changing the control model for feedforward control of the side stream influences the cycle time and the separating cost (performance criteria). We present a new control model, referred to as the Modified-Ideal Side draw Recovery arrangement (Modified-ISR) for feedforward control, which is compared with the status quo in terms of the performance criteria. We found that the proposed control model is superior, in terms of generating lower cycle time cycles and thus SC, compared to the state of the art. Further, we analyze the effects of altering the type of controller used in its feedback implementation. Furthermore, an optimization-based procedure for finding a better side stream flow rate trajectory (during a cycle) is presented. We found that attempts in using rigorous dynamic optimization to improve upon the control trajectories provided by the Modified-ISR framework improved neither the SC nor the cycle time relative to the Modified-ISR case.

2. Side stream feedforward control

2.1 Ideal side draw recovery arrangement

The rationale for the control of the side stream flow rate was to reduce the loss of intermediate boiling component from the distillate and bottoms streams (Adams and Seider, 2008). The feedforward control model required was derived from the component B column mass balance by assuming that the column is operated at a pseudo-steady state at any given time (t), which is:

$$F(t)x_{MV,B}(t) = S(t)x_{S,B}(t) + Di(t)x_{Di,B}(t) + Bo(t)x_{Bo,B}(t) \quad (4)$$

where, $x_{S,B}(t)$ is the mole fraction of component B in the side stream, $x_{Di,B}(t)$ is the mole fraction of component B in the distillate stream, and $x_{Bo,B}(t)$ is the mole fraction of component B in the bottoms stream.

In the ideal case, there would be no loss of intermediate boiling component either through the distillate stream or the bottoms stream at any given time. In addition, none of the light or heavy species would exit through the side draw. Therefore, $x_{Di,B}(t)=x_{Bo,B}(t)=0$, and $x_{S,B}(t)=1$, thus resulting in the ideal side draw recovery arrangement (ISR) control model, represented by Eq (5), where $S_{ISR}(t)$ is the model-defined side stream flow rate.

$$S_{ISR}(t) := F(t)x_{MV,B}(t) \quad (5)$$

In practice however, the feedforward-side stream control is implemented through feedback control of the side stream, where $S(t)$ (output) is made to track $S_{ISR}(t)$ (setpoint), which will be henceforth referred to as "ISR feedback control". A proportional (P) controller was normally used to manipulate the side stream control valve ($v_s(t)$) to try to get the actual flow rate to track the ISR-defined flow rate setpoint (Pascall and Adams, 2013).

The ISR control model used in the Pascall-Adams control configuration has consistently shown to be effective in achieving good cycle performance and cycle stability in many studies (Ballinger

and Adams, 2017; Meidanshahi et al., 2017; Meidanshahi and Adams, 2016, 2015, Pascall and Adams, 2014, 2013; Wijesekera and Adams, 2015a, 2015b). The derived control model defines an output trajectory, $S(t)$, based on the control input, $F(t)$, the state, $x_{MV,B}(t)$, and the choice of the controller tuning parameters. However, the previous studies also used optimization to find the optimal control system design (which included the tuning parameters for the P controller tracking the $S_{ISR}(t)$). Although this was not discussed much in those works, an analysis of the results shows that controller configurations which did not track $S_{ISR}(t)$ closely were economically superior than those that tracked $S_{ISR}(t)$ very closely. Thus, there is evidence that better models could be found for $S_{ISR}(t)$.

2.2 Modified-ideal side draw recovery feedforward control model

Although the ISR model for side stream control has had good demonstrable performance characteristics, simulations have shown that $x_{S,B}(t)$ is often far from unity early in the cycle. Furthermore, the variable's value is never exactly 1.0 at any time throughout a cycle and the variation in $x_{S,B}(t)$ is large during the semicontinuous cycles. Thus, designing a feedforward control model by considering $x_{S,B}(t)$ as unity is far from reality. Hence, the proposed feedforward control model is designed without using the assumption of a perfectly pure side draw, with Eq. (4). now reducing to the Modified Ideal Side Draw Recovery (Modified-ISR) arrangement. The new model defines, at each time instance, the amount of component *B* recycled to the MV through the side stream as opposed to the ISR model. In Eq. (6), $S_{MISR}(t)$ is the side stream flow rate as defined by the new model:

$$S_{MISR}(t) \coloneqq \frac{F(t)x_{MV,B}(t)}{x_{S,B}(t)} \tag{6}$$

Since $x_{S,B}(t) \in [0\ 1]$, comparing Eq. (5). and Eq. (6)., $S_{MISR}(t)$ is higher in value than $S_{ISR}(t)$ at instances where there is no difference in the values of $F(t)$ and $x_{MV,B}(t)$. The positive trade-off of using the Modified-ISR model therefore might be that the total cycle time could potentially be lower relative to using the ISR arrangement because the MV can be enriched with component *B* faster. The side stream will contain some amount of components *A* and *C* and thus, on the negative side, the approach could be essentially counter-productive by collecting too much of the heavy and light species in the side draw, thus making overall recovery times longer. An added concern with using the Modified-ISR model is the need for an additional on-line composition measurement of component *B* in the side draw. In this study, since we deal with an ideal-case analysis, the cost and measurement noise of the additional composition sensor is neglected. However, a 3-minute dead time associated with this additional composition sensor was considered.

The side stream feedforward control using the Modified-ISR control model was implemented using a feedback loop, where the setpoint of the controller in the loop was varied according to the model just like the ISR feedback control. The present study aims to understand the changes in

process dynamics when using the ISR and Modified-ISR feedback control approaches and its effect on economic performance

3. Simulations using the sequential design methodology

The effect of changing the feedforward control model was studied extensively through the simulation of four semicontinuous ternary distillation systems, named, I, II, III, IV (with different feed mixture compositions and chemical components), and semicontinuous multicomponent distillation of a four-component mixture (V). These are shown in Table 1.

Table 1 The five semicontinuous distillation systems considered in this work. Feed compositions are given in mole fraction. Stages includes the condenser and reboiler in the column and the column trays (with an assumed 75% tray efficiency), with stage 1 being the condenser. Feed stages are above stage, and side stream stages are on-stage (liquid phase). $F(t)$ at time $t = 0$ (around which the column is *sized*) is represented as $\overline{F}$, and $S(t)$ at time $t = 0$ is represented as $\overline{S}$.

System	Feed Mixture	Upstream Feed Composition				Stages	Stage Location		$\overline{F}$ (kmol/h)	$\overline{S}/\overline{F}$
		$x_{A,F}$	$x_{B,F}$	$x_{C,F}$	$x_{D,F}$		*Feed*	*Side stream*		
I	BTX	0.2	0.6	0.2	-	40	25	14	100	0.655
II	BTX	0.33	0.33	0.34	-	40	25	14	100	0.39
III	BTX	0.4	0.2	0.4	-	40	25	14	100	0.25
IV	DME, MeOH, H_2O	0.82	0.14	0.04	-	25	13	12	12.64	0.149
V	C_6, C_7, C_8, C_9	0.25	0.25	0.25	0.25	50	24, 25	15, 36	37.81	0.25, 0.25

Systems I to III represent the separation of an almost ideal but industrially relavent ternary mixture of benzene, toluene and o-xylene (BTX), where toluene is the intermediate boiling component (B). The differences between the three systems is the concentration of toluene in the feed to the MV, with system I having the highest and system III having the lowest. System IV represents the ternary separation of dimethyl ether (DME), methanol (MeOH), and water (H_2O), which was extensively studied by Pascall and Adams (2013) because of the importance of biomass-based DME production as an alternative fuel source to diesel. These systems were specifically chosen because they were well-studied in the semicontinuous distillation literature and are illustrative of the zeotropic separations of ternary systems. System V provides a basic example of the separation of four components (alkanes-C_n, n = 6 to 9) used in the study by Wijesekara and Adams (2015). Quaternary semicontinuous distillation is carried out using one column and two middle vessels. Therefore, two side streams are recycled to the two MVs for separating the two intermediate

boiling components. In this case, components *B* (heptane) and *C* (octane) are both intermediate boiling components, each recovered in a separate MV, while component *D* (nonane) is the bottoms product.

3.1 Remarks on the initial state

The design methodology adopted is the same as the one described and used by Pascall and Adams (2013) in their study, which we call the "sequential design methodology". The idea in this approach was to initially identify a "hypothetical" steady-state which is used as the initial state for dynamic simulation. At this initial state, the distillate and bottoms products are separated at the desired purities, while the side stream is not yet recycled to the MV. This state is a reasonably good approximation of the beginning of the separating mode (Wijesekera and Adams, 2015a) noting that the actual state cannot be predicted *a priori*. The steady state side stream flowrate ($\bar{S}$) can be chosen according to the ISR feedforward control model, however, this can be low enough to cause flooding in the column. Therefore, generally a slightly higher value than the ISR specified value is chosen to avoid flooding within the column at this state.

Data required for column design at the initial state, such as number of stages, feed stage location, side draw location, column pressure, pressure drop across stages (ΔP) and product composition were taken from Ling and Luyben (2009), Pascall and Adams (2013), Wijesekara and Adams (2015), and Meidanshahi and Adams (2015) (see Table 1 and Table 2). The thermodynamic properties of systems I to III were calculated using the Non-random two-liquid (NRTL) activity coefficient model (Ling and Luyben, 2009). This model was validated to match well with experimental data for the isobaric state of 101.325 kPa, where the R^2 value was approximately 0.99 for each binary interaction. The experimental data were taken from Gupta and Lee (2013, 2012). The vapor liquid equilibrium was modeled using the Peng Robinson-Wong Sandler-UNIFAC model and the UNIQUAC-Redlich Kwong model when simulating systems IV and V respectively (Pascall and Adams II, 2013; Wijesekera and Adams II, 2015a). These models were not validated against experimental data in this study since it was already verified in the respective studies.

Table 2 Column conditions at the initial state.

System	Mole Purity of Each Product Stream at the Initial State				Condenser *P*	Tray Δ*P*	Flooding
	A	B	C	D	**(atm)**	**(atm)**	*Initial State*
I	0.99	0.91	0.99	-	0.37	0.0068	No
II	0.99	0.83	0.99	-	0.37	0.0068	No
III	0.99	0.77	0.99	-	0.37	0.0068	No
IV	0.9995	0.96	0.9905	-	10	0.0068	No
V	0.95	0.95*	0.93*	0.95	1	0.0068	No

In systems I to III, the MV was sized to have a total molar hold-up of 200 kmol of liquid feed, and in systems IV and V, the MV was sized to have a total molar hold-up of 100 kmol of liquid feed using the design heuristics applied by Pascall and Adams (2013). The reflux drum and the sump were sized according to the design heuristics of Luyben (2006). It was verified that flooding and weeping constraints were met at the initial state (see Table 2).

The total direct costs for the systems were calculated in $US2016 using Aspen Capital Cost Estimator V10 (Aspen Technologies). The utility costs of steam and cooling water were the only operating costs that were considered in the calculation of *SC* because they constitute the major portion. The methodology as provided by Towler and Sinnott (2013) was used to estimate the cost of steam and cooling water based on energy market prices. A natural gas price of 2.64 $/GJ (U.S. Energy Information Administration, 2017) and electricity price of 0.097 $/kW (IESO) was used for the estimation of cooling water and steam costs.

3.2 Comments on control

The Pascall-Adams control configuration was used for the purposes of controlling the desired outputs at the chosen setpoint values. The concentration controllers maintain the distillate and bottoms product concentrations at the chosen initial state values, which are perceived as the integral average purities (during the cycle) of these products. Similarly, the level controllers maintain the reflux drum and sump levels at the respective initial state values.

PI controllers were used for concentration and level control in the simulations. The controllers are initially tuned manually such that the integral squared errors of the distillate and bottoms concentrations are minimized (Pascall and Adams, 2013). The ISR and Modified-ISR feedback control uses reverse acting P or PI controllers for setpoint tracking.

Although the Pascall-Adams control configuration was used in quaternary semicontinuous distillation, it is more intricate compared to the ternary case (see Figure 3). In the quaternary case,

there are two feed inlets to the column from the two MVs, and therefore the reflux drum level is controlled by manipulating the two feed flow rates collectively as illustrated by Wijesekera and Adams, (2015a). Furthermore, in their study, both the side streams where controlled using the ISR feedforward control model as follows (Wijesekera and Adams, 2015a):

$$S_{ISR,1}(t) \coloneqq F_1(t)x_{MV1,B}(t) + F_2(t)x_{MV2,B}(t) \tag{7}$$

$$S_{ISR,2}(t) \coloneqq F_1(t)x_{MV1,C}(t) + F_2(t)x_{MV2,C}(t) \tag{8}$$

where $S_{ISR,i}(t)$ is the model specified setpoint of the side stream flow rate of stream i, $F_i(t)$ is the feed stream to the column from the i^{th} MV, $x_{MVi,B}(t)$ and $x_{MVi,C}(t)$ are mole fractions of components *B* and *C* in the feed stream *i* to the column. The Modified-ISR control model for controlling the two side streams can be similarly defined as follows:

$$S_{MISR,1}(t) \coloneqq \frac{F_1(t)x_{MV1,B}(t)}{x_{S1,B}(t)} + \frac{F_2(t)x_{MV2,B}(t)}{x_{S2,B}(t)} \tag{9}$$

$$S_{MISR,2}(t) \coloneqq \frac{F_1(t)x_{MV1,C}(t)}{x_{S1,C}(t)} + \frac{F_2(t)x_{MV2,C}(t)}{x_{S2,C}(t)} \tag{10}$$

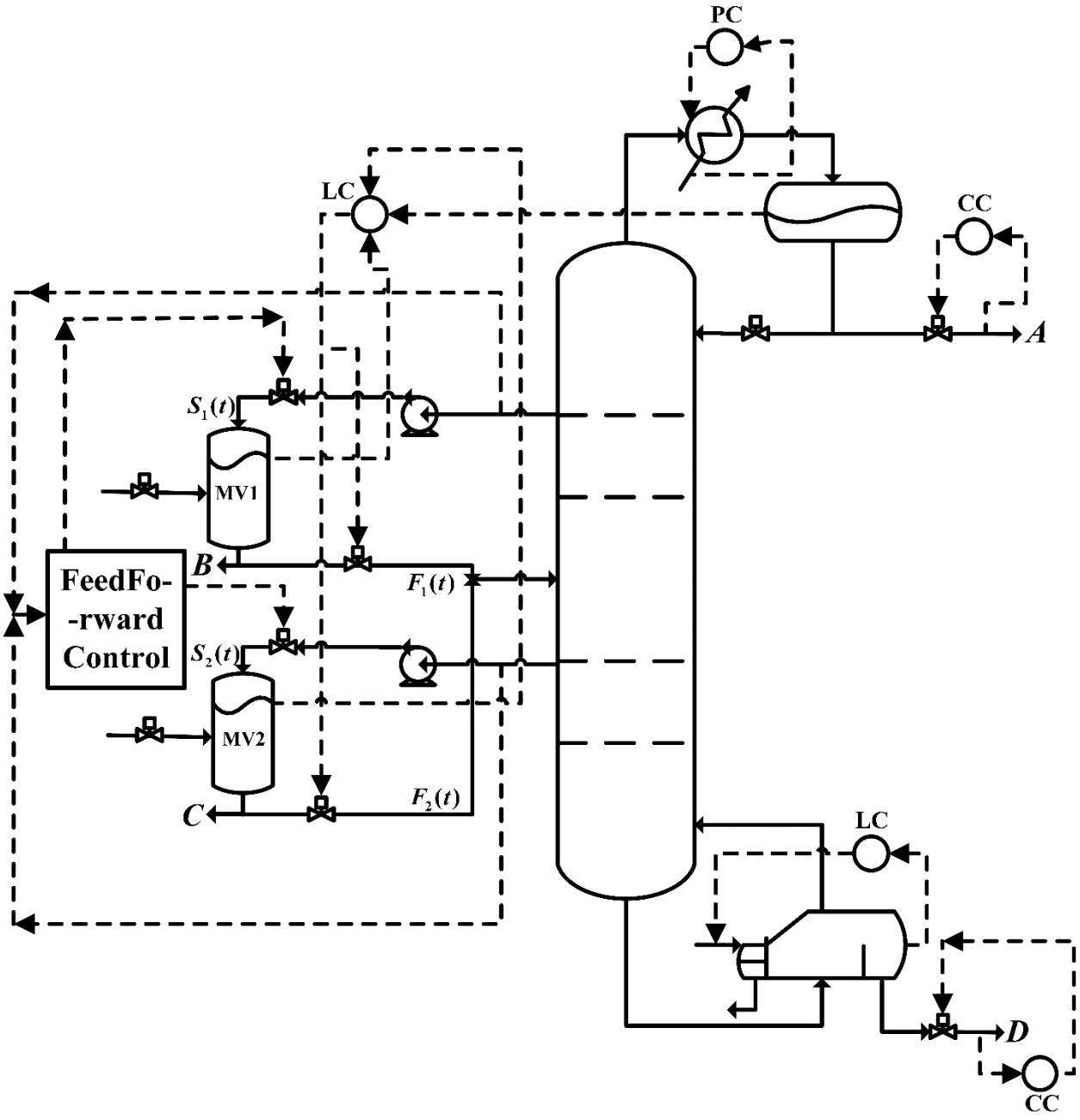

Figure 3: Control structure as suggested by Wijesekara and Adams, 2015 for quaternary semicontinuous distillation

3.3 Controller tuning

The tuning parameters of the controllers are design degrees of freedom in semicontinuous distillation, whose choice will generate different control trajectories and thus different converged cycles from the same initial state. Optimal controller tuning parameters were therefore found with

the objective of minimizing SC subject to constraints by using dynamic optimization. The decision variables include tuning parameters of the distillate concentration controller, bottoms concentration controller and side stream flow rate controller (represented as elements in the vector $[K_{Di}\ \tau_{Di}\ K_{Bo}\ \tau_{Bo}\ K_S\ \tau_S\ ]^T$) with manually tuned values of these variables used as the initial guess.

It should be emphasized here that the improved designs found were sub-optimal because integer decision variables such as diameter of the column, number of stages etc., were not included. Hence, for the sake of being rigorous, the design obtained through dynamic optimization is called the "improved" design and the tuning parameters are referred to as "improved" rather than "optimal". Integer design degrees of freedom were not included during optimization because of the complexity and large computational time required to find a local optimal solution (Meidanshahi and Adams, 2016). Also, since finding the optimum of each system is not the objective of the present study, a much simpler method was preferred. For details on the procedure to find an optimal semicontinuous design by including the integer design variables refer to Meidanshahi and Adams (2016).

The improved semicontinuous distillation design was found using the Aspen Dynamics dynamic optimization tool (Aspen Technologies), which uses the control vector parametrization approach. Using this tool, the controller tuning parameter values that allow the systems to converge to the best possible cycles from the respective initial states were found. Endpoint constraints were used to ensure that the average purity constraints of the distillate and bottoms streams were met. The height of liquid in the middle vessel was ensured to be close to the initial value ($|h_{MV}(t_f) - h_{MV}(t_i)| \leq \epsilon$) at the end of each cycle so that the system is periodic.

The dynamic simulation of each system is run for ten cycles from the initial state because it usually takes a few cycles for the system to converge to a stable cyclic steady state starting from the hypothetical steady state, and ten cycles is sufficiently large to obtain a cyclic steady state in all circumstances. Thus, the 10th cycle is used to compute the SC of the system as a whole as follows:

$$SC = \frac{\frac{Total\ Direct\ cost}{3\ years} + \left(\frac{w}{t_f - t_i}\right)\int_{t_i}^{t_f}(C_r Q_c(t) + C_s Q_r(t))\ dt}{\left(\frac{w}{t_f - t_i}\right)\int_{t_i}^{t_f}(Di(t))dt} \tag{11}$$

where C_r is the cost of the refrigerant, C_s is the cost of low pressure saturated steam, t_i and t_f are the initial and final times of the 10th cycle in hours, and $\left(\frac{w}{t_f - t_i}\right)$ is the number of cycles in a year assuming w working hours per year. The optimization problem formulation is:

$$\underset{K_j,\ \tau_j,\ t_f}{minimize} \quad \text{SC}$$

subject to Mass Balance Constraints
Energy Balance Constraints

Momentum Balance Constraints
Equilibrium Relationships
All other model equations

$$h_{MV}^{l}(t_f) \le h_{MV}(t_f) \le h_{MV}^{u}(t_f)$$

$$x_{Di,A}{}^{l} \le \langle x_{Di,A} \rangle \le x_{Di,A}{}^{u}$$

$$x_{Bo,C}{}^{l} \le \langle x_{Bo,C} \rangle \le x_{Bo,C}{}^{u}$$

$$K_j^l \le K_j \le K_j^u$$

$$\tau_j^l \le \tau_j \le \tau_j^u$$

$$t_f^l \le t_f \le t_f^u$$

where t_f is the final cycle time, with t_f^l and t_f^u being the lower and upper bounds of final cycle time respectively. Lower and upper bounds of other variables are defined analogously. The integral average mole fraction of A in the distillate stream, $\langle x_{Di,A} \rangle$, is defined as:

$$\langle x_{Di,A} \rangle := \frac{\int_0^{tf} x_{Di,A}(t) Di(t) dt}{\int_0^{tf} Di(t) dt} \tag{12}$$

where $x_{Di,A}(t)$ is the mole fraction of benzene in the distillate stream at time *t*. The integral average mole fraction of B in the bottoms stream, $\langle x_{Bo,C} \rangle$, is defined analogously. Here, K_j represents the proportional gain of the j^{th} PI controller, τ_j represents integral time constant of j^{th} PI controller, where $j =$ (Distillate) *Di,* (Bottoms) *Bo,* (Side Stream) *S.*

4. Simulation results and analysis

4.1 Ternary systems

The changes in the evolution of the system from the initial state when using the ISR and Modified-ISR feedback control is analyzed in detail by using system II as an example. It is later demonstrated that the analysis is consistent in all other systems under study including the quaternary system.

4.1.1 ISR feedback control of side stream flow rate

ISR feedback control was first implemented using a P controller (ISR feedback-P) in the simulation studies conducted on system II. Improved tuning parameter values were obtained from optimization of the system. From the initial state (represented as a circle in Figure 4), the system evolved and converged to a periodic orbit (illustrated in the phase plane plot in Figure 4). To generate the phase plane plot, the system's state variables, the molar hold up of component B on the side draw tray $M_{B,S}(t)$ and the molar hold up of component B on the feed tray $M_{B,F}(t)$ are chosen, because they are directly affected by $S(t)$ and $F(t)$ respectively. The orbit represented in Figure 4 was traced for ten cycles by employing the improved controller tuning parameters. In the absence of any state dependent inputs that trigger a mode transition (i.e., if the system is run in

separating mode without stopping), the system will be attracted to an equilibrium point (ε, the solid point). The point α is the end of the separating mode (and beginning of the discharging mode), where the concentration of toluene (component *B* in system II) in the MV reaches the desired purity value, in this case 0.99. α is close enough to ε that they are indistinguishable in Figure 4. The change in the column's state during the discharging mode is not significant and hence the end of the discharging mode cannot be distinguished clearly from point α or the equilibrium point on the phase plane plot. However, during the charging mode the values of the selected variables vary substantially, moving the system from point α to point β, which signifies the end of the charging mode and the beginning of a new separating mode.

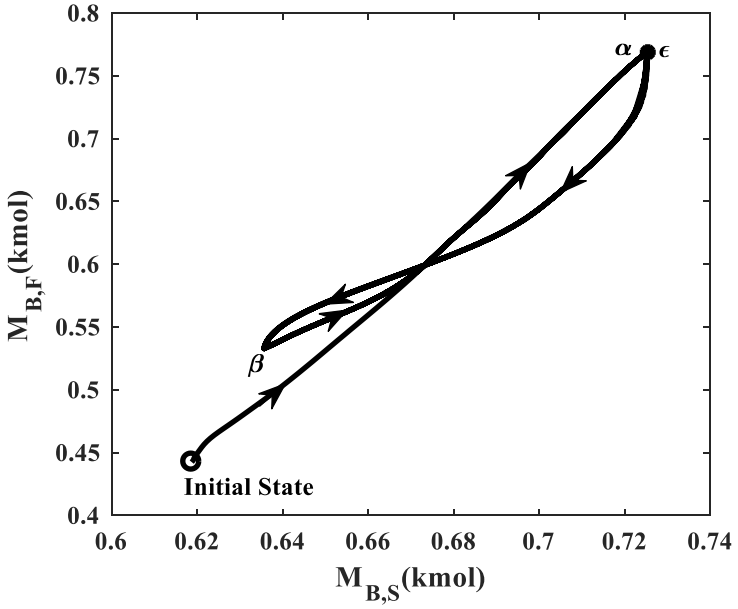

Figure 4: Phase plane plot (includes 10 cycles) which illustrates the evolution of the system when the improved ISR feedback-P control for side stream flow rate is used. The circle indicates the initial state of the simulation.

In Figure 5, the setpoint tracking ability of the P controller using the improved tuning parameter values is presented. As illustrated for three representative cycles, by using the improved tuning parameters values the setpoint was not tracked exactly. Therefore, to understand the implications of tracking the ISR-defined setpoint as closely as possible, different controller tuning parameter values were manually chosen (called the "setpoint tracking" tuning parameter values). The cycle time and the SC were found to be greater, as expected, by tracking the setpoint closely. The cycle times were higher because the side stream valve was closed significantly during the charging mode (lower toluene concentration in the column feed) and thus having lower recycle rates during that period. Also noticeable from Figure 5 is that the side stream flow rate trajectories are completely different in the improved and setpoint tracking cases. Therefore, by changing the tuning parameter values different control trajectories ($v_s(t)$) are generated.

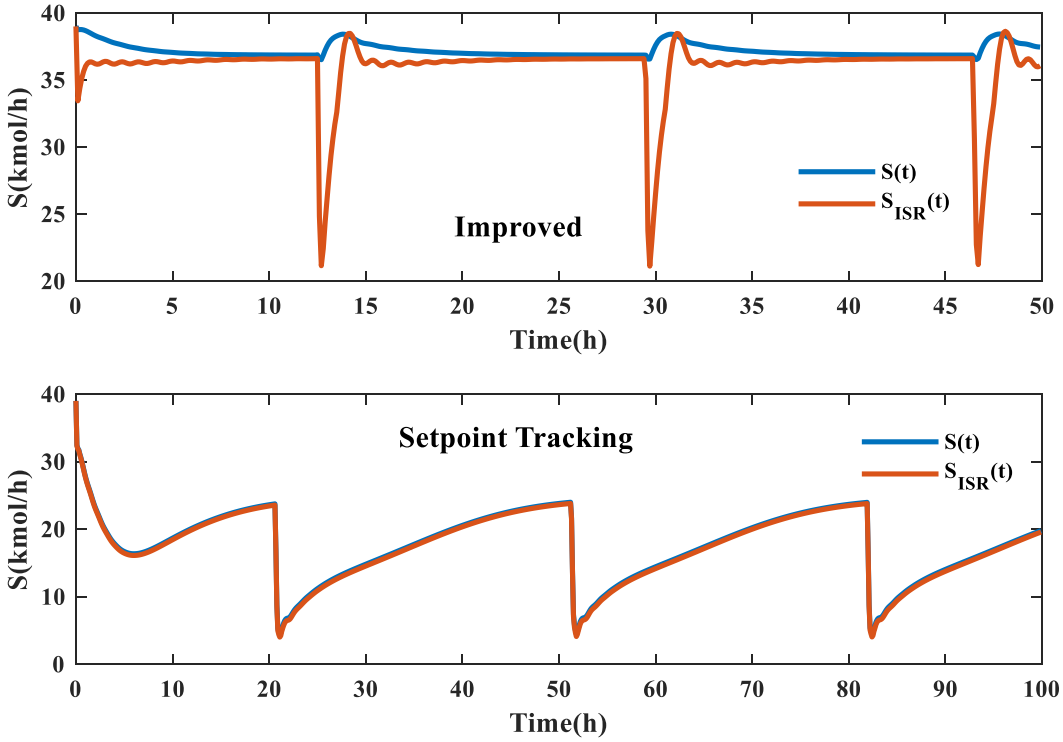

Figure 5 Illustration of $S(t)$ vs $S_{ISR}(t)$ when the setpoint tracking or improved tuning parameter values are used to simulate system II. The ISR feedback-P control is used.

Another approach to track the setpoint exactly is to use a PI controller (ISR feedback-PI) instead of a P controller. By changing the type of controller in the feedback loop to track the ISR-defined setpoint, it was found that the system essentially failed (Figure 6), with the feed and side draw rates dropping to zero and the column entering total reflux mode. After close examination, it was observed that the side stream valve was fully closed because of a large integral error. The reason for this huge integral error is possibly due to the choice of the initial state. As stated previously, $\bar{S}$ is chosen to be at a slightly higher value than the ISR specified value at the initial state. Therefore, in ISR feedback loop there is a negative error ($(S_{ISR}(0) - \bar{S}) < 0$), which the controller tries to compensate by closing the valve (v_s). The integral term of the PI controller accumulated this negative error during the cycle(s) and gradually closed the side stream flow control valve fully. Simultaneously, the concentration of toluene in the distillate and bottoms streams was observed to be increasing due to the side stream valve closure, thus eventually leading to the shutting of distillate and bottoms flow control valves. At the same time, to maintain the reflux drum level the feed flow control valve to the column was closed thus resulting in the total reflux state column operation. This type of dynamic behaviour is undesirable for semicontinuous distillation and so the ISR feedback-P is the appropriate choice. Note that, in all prior semicontinuous studies using the ISR control model, a P controller was used instead of PI, likely for the same reason.

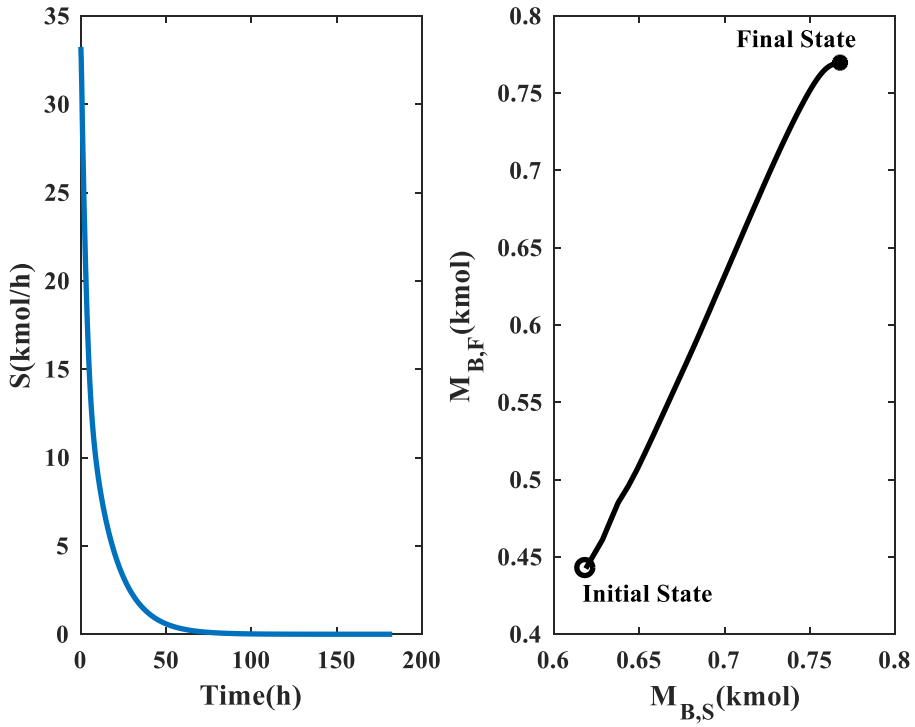

Figure 6. The evolution of $S(t)$, flow rate of side stream recycled to the middle vessel (kmol/h) with time and the phase plane plot illustrating the effect of using the ISR feedback-PI control for side stream flow rate. The system approaches the failure (total reflux) state.

4.1.2 Modified-ISR feedback control of side stream flow rate

To follow the same natural progression followed in the previous section, the Modified-ISR feedback control was also first implemented with the aid of a P controller (Modified-ISR feedback-P) in the simulation studies conducted on system II. The tuning parameters were initially found manually so that the integral squared error was reduced and the Modified-ISR setpoint was tracked. The cycle time of the converged periodic orbit and the SC were then compared with improved ISR feedback-P and were found to be only marginally lower (~0.004%). Setpoint tracking was found to be difficult in the case of Modified-ISR feedback-P because of numerical convergence issues encountered during the simulation. However, when a PI controller was used in the Modified-ISR feedback control loop (Modified-ISR feedback-PI), even before the optimization step was performed, T and SC were found to be significantly lower (~12% and ~13% respectively) than the manually tuned Modified-ISR feedback-P case, and the failure state was not reached. Thus, the optimization step was not carried out for the Modified-ISR feedback-P case. The reason for the lower T and SC in the Modified-ISR feedback-PI case is because of the positive error accumulated by the integral term of the PI controller, which is again due to the choice of the initial state. It is well known that, $\bar{\delta} \equiv \overline{Di}\bar{x}_{Di,B} + \overline{Bo}\bar{x}_{Bo,B}$ (variables with over bar indicate steady state values) in Eq.(4), is not equal to zero in reality at steady state; unlike in the derivation of the Modified-ISR model. Thus, from Eq. (4) and Eq. (6),

$$\bar{S} = S_{MISR}(0) - \frac{\bar{\delta}}{\bar{x}_{S,B}}$$

Since $\frac{\bar{\delta}}{\bar{x}_{S,B}}$ is positive, $\bar{S}$ is less than $S_{MISR}(0)$, thus resulting in positive error ($(S_{MISR}(0) - \bar{S}) > 0$). Therefore, the side stream control valve is opened by the controller at the initial state to compensate for the error unlike the ISR case. The integral term accumulates this error to open the side stream valve fully for a certain length of time during the stable cycle (Figure 7). Although, this occurs because of the integral windup, there is a natural anti-windup (even though it does not completely reset the integral term) process happening during the charging mode of the cycle. This is because the concentration of *B* is lower in the MV during this mode and thus reducing the value of the model predicted setpoint. Further, it was found that when using the improved tuning parameter values in Modified-ISR feedback-PI case, the process variable tracks the setpoint (Figure 8) for the later portion of the cycle but does not quite track it during the earlier portion of the cycle. Thus, in general, the feed forward models in combination with side draw controller tuning parameters together act as control (v_s) trajectory generators that guide the system to reach different periodic orbits (stable cycles) in the phase space.

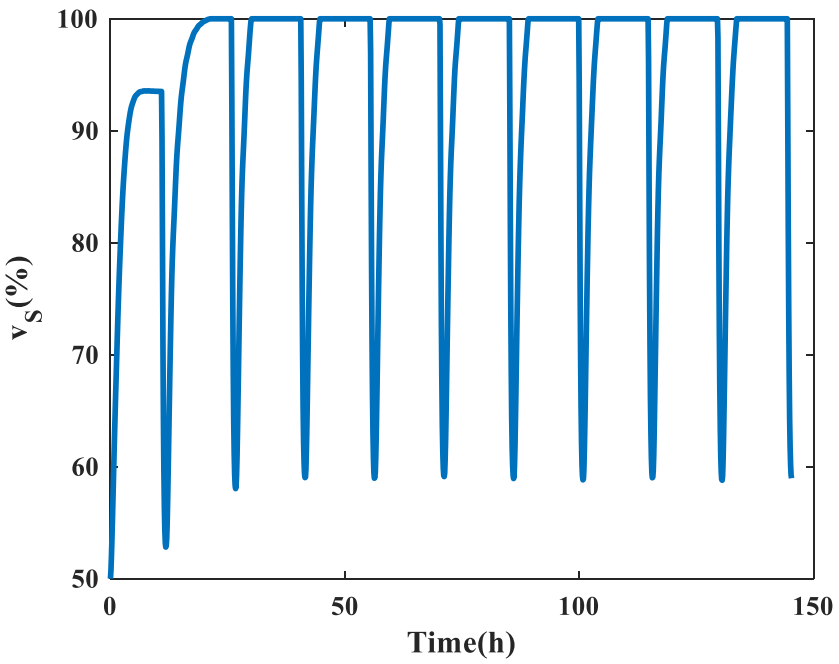

Figure7: Side stream valve opening as a function of time when improved Modified-ISR feedback-PI control is used in system II.

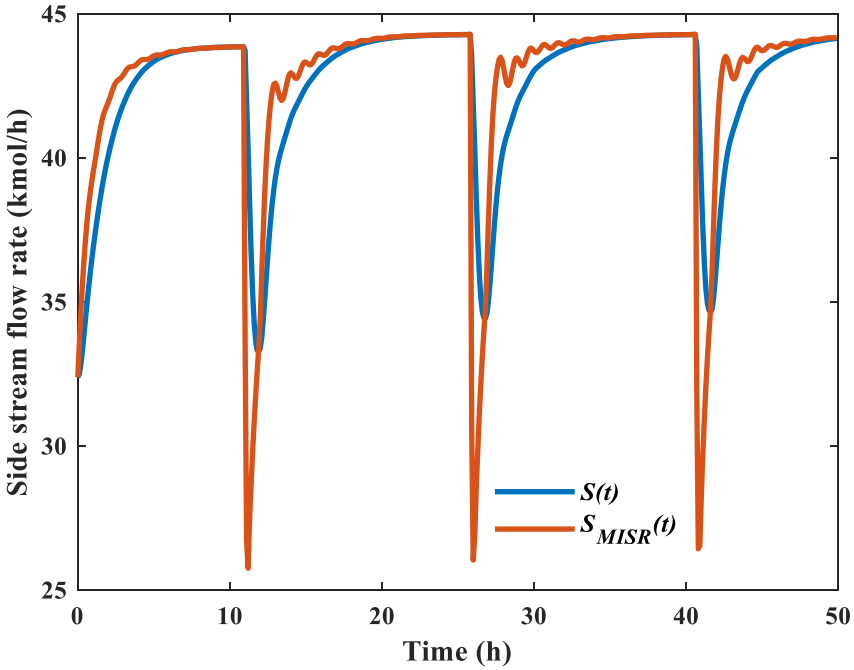

Figure 8 Illustration of process variable not tracking the setpoint when the improved tuning parameter values are used to simulate system II. The Modified-ISR feedback control is used.

The improved periodic orbit to which the system converged in the Modified-ISR feedback-PI controller case is traced in (Figure 9) and is quantitatively slightly different from the improved periodic orbit of the ISR feedback-P case (Figure 4). This is because the set of side stream valve opening trajectories that can be generated in the former case is different from the latter. Furthermore, it is evidently noticeable that it takes a few semicontinuous cycles to approach the basin of attraction of the periodic orbit unlike the ISR case.

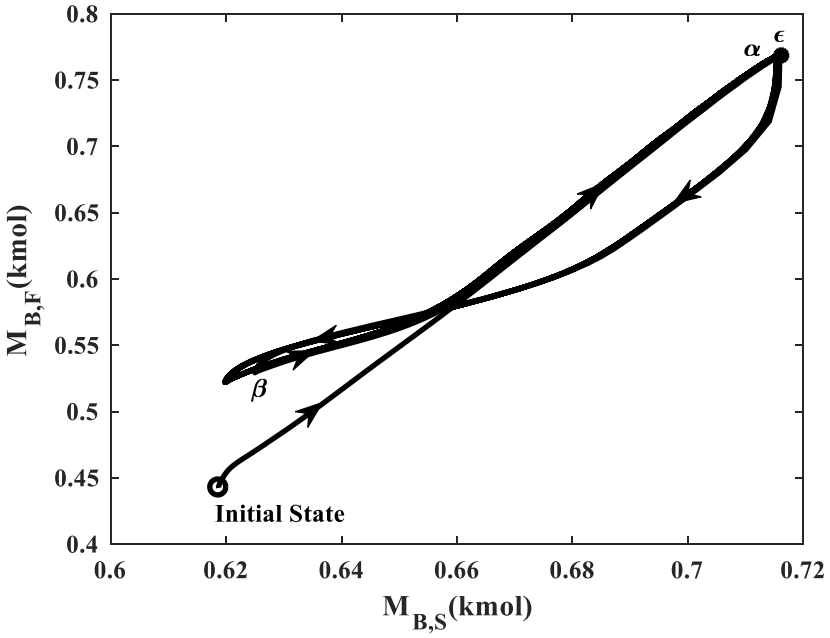

Figure 9: Phase plane plot (includes 10 cycles) which illustrates the evolution of the system when the improved Modified-ISR feedback-PI control for side stream flow rate is used. The circle indicates the initial state of the simulation.

The side stream flow rate ($S(t)$) at any given time in a stable cycle when using the Modified-ISR feedback-PI control is greater than when using the ISR feedback-P control. Consequently, the cycle time is decreased considerably in the former when compared to the latter because the middle vessel reaches the desired purity in a reduced amount of time. Thus, the frequency at which batches of feed are processed is higher simultaneously leading to reduced SC (results presented in section 4.3). Furthermore, it was observed that there was no column flooding (Figure 10) or weeping during the dynamic operation and the distillate and bottoms product purities are maintained at the desired values.

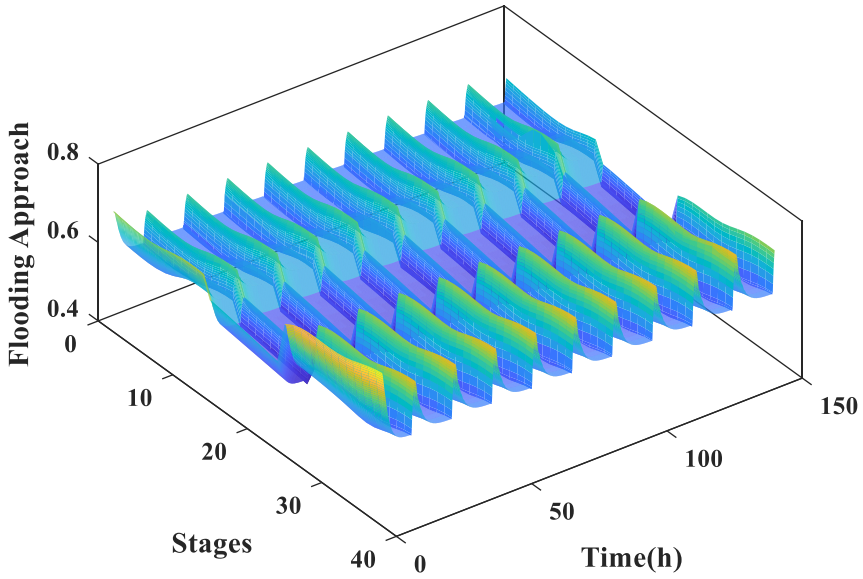

Figure 10 Illustration of flooding approach profile in system II for 10 cycles. Modified-ISR feedback-PI control was employed.

4.1.3 Comparison of separating costs

The cycle time when using the Modified-ISR feedback-PI control to control the side stream flow rate in system-II is almost 12.5% lower when compared to the cycle time when using the ISR feedback-P control. Similarly, the SC when using the latter approach is substantially lower (by almost 13%) when compared to the former approach (Table 3). The Modified-ISR feedback-PI control resulted in a 13% reduction in SC for the same total direct cost, which is a remarkable improvement in SC and is even significantly bigger than the benefits of finding the improved tuning parameters. Thus, the Modified-ISR feedback control with PI controller must be fundamentally better in terms of separating the mixture faster when compared to the state of the art.

Table 3 The cycle time and the separating cost comparisons in system II. Cycle Time is the time taken to complete the 10^{th} cycle.

Control	***T* (h)**	***SC*** **($/kmol of product produced)**	**% decrease in SC compared to ISR feedback-P**
Improved ISR feedback-P	16.97	8.25	-
Improved Modified-ISR feedback-PI	14.83	7.16	13.21
No Control ($v_s(t) = 100\%$)	14.82	7.25	12.12

Since the Modified-ISR feedback-PI control has the lowest SC, and because the side stream valve was saturated during the cycle, perhaps the side stream control valve could be fully opened all the time instead of using either ISR or Modified ISR. This was tested and was found that the cycle time was slightly lower, but the SC was slightly worse compared to the improved Modified-ISR case (Table 3). This could be because of two reasons: (1) the loss of intermediate boiling component through the distillate and bottoms streams, and (2) higher heat duties because of higher amount of component *B* in the feed at any given time.

While the results imply that the Modified-ISR control model generates a $S(t)$ trajectory that leads to better cycles in terms of *SC* than the ISR control model, the generality of the above analysis and the relevant conclusions are presented next.

4.1.4 Comparison of ISR and Modified-ISR feedback control in other ternary systems

The analysis in the previous sections is found to be consistent even for other ternary systems, namely, I, III, and IV. The dynamic behavior of the systems changed as the tuning parameter values were altered. As an example, Figure 11 illustrates the change in the periodic orbit when improved and setpoint tracking tuning parameters are used in ISR feedback-P control. Furthermore, in all systems that were studied, the setpoint was not tracked exactly when the improved tuning parameters were employed.

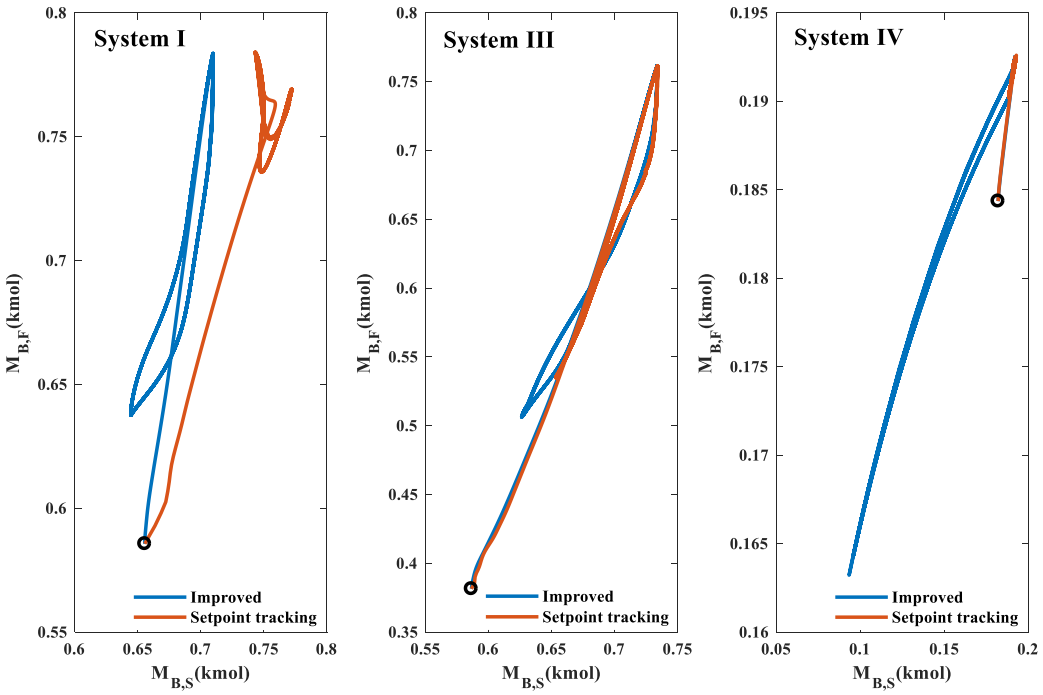

Figure 11 Phase plane plots to illustrate the dynamic behaviour because of using the ISR feedback-P control (systems I, III, IV). The open circle indicates the hypothetical steady-state (used as the

initial state). "Improved" indicates that the side stream controller tuning parameters are found using optimization and "Setpoint tracking" implies that the side stream controller tuning parameters were manually selected to nearly closely track the setpoint.

The same undesirable behavior of reaching the total reflux state was observed when the PI controller was used in ISR feedback control in all cases. Also, Modified-ISR feedback-P control with controllers manually tuned for minimizing integral squared error is only marginally better than improved ISR feedback-P control in all three simulated cases (Table 4).

Table 4 The cycle time and separating cost comparisons for the systems under study. Cycle Time is the time taken to complete the 10^{th} cycle. * The side stream flow rate function is highly oscillatory during the cycle. § Status-quo side stream flow rate control.

	System I	**System II**	**System III**	**System IV**	**System V**
Cycle Time (T) (h)					
ISR feedback-P control - Setpoint tracking	27.52	30.81	34.44	95.28*	6.31
ISR feedback-P control - Improved§	14.36	16.97	18.87	65.19	4.60
Modified ISR feedback - P control – Manually tuned (K_s = 0.1 (%/%))	13.31	16.90	18.85	64.26	4.63
ISR feedback - PI control	-	-	-	-	-
Modified ISR feedback - PI control-Improved	12.79	14.83	16.36	55.62	4.08
Dynamic Optimization	12.79	14.51	16.12	55.00	-
Separating Cost (SC) ($/kmol of product produced)					
ISR feedback-P control – Setpoint tracking	24.60	15.95	14.62	21.16	29.70
ISR feedback-P control - Improved§	12.37	8.25	7.57	21.16	21.77
Modified ISR feedback - P control - Manually tuned (K_s = 0.1 (%/%))	11.40	8.25	7.57	20.00	21.62
ISR feedback - PI control	-	-	-	-	-
Modified ISR feedback - PI control - Improved	10.93	7.16	6.49	17.35	18.50
Dynamic Optimization	10.92	7.00	6.39	17.10	-

With improved Modified-ISR feedback-PI control, the periodic orbit (Figure 12) traced with the improved tuning parameter values is slightly different from the periodic orbit of improved ISR feedback-P control (Figure 11) for systems I, III and IV.

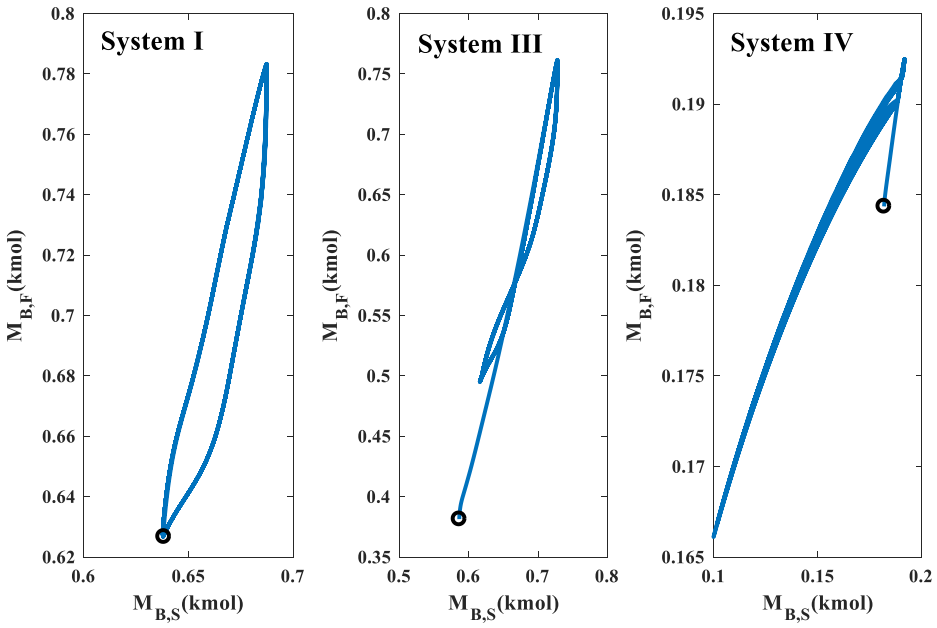

Figure 12 Phase plane plots to illustrate the dynamic behaviour because of using the improved Modified-ISR feedback-PI control (systems I through IV). The open circle indicates the hypothetical steady-state (used as the initial state).

When using the improved Modified-ISR feedback-PI control to control the side stream flow rate, the cycle time was almost 10% to 15% lower when compared to the improved ISR feedback-P control. Similarly, the SC also is substantially lower by almost 10% to 19% when compared to the status quo. Therefore, from an economic perspective (Table 4), the Modified-ISR feedback-PI control is better than the state of the art in all cases. Thus, the proposed feedforward model for side stream control is better to reach periodic orbits (stable cycles) with lower SC than the ISR feedforward control model.

4.2 Quaternary systems

Interestingly, the conclusion of the analysis carried out thus far for ternary systems also holds true for the more complicated quaternary system (system V). Both the side streams when controlled using the control models as defined in Eq. (9) and Eq. (10) (Modified-ISR control model for the quaternary system) confirmed similar results. As an example, Figure 13 demonstrates that the periodic orbits are qualitatively different when a different side stream control is applied. This illustrates the scalability in the functionality of the proposed control model for the distillation of mixtures with *n*-components using "*n*-2" MVs semicontinuously while resulting in lower SC cycles (see Table 4) compared to the current state of the art.

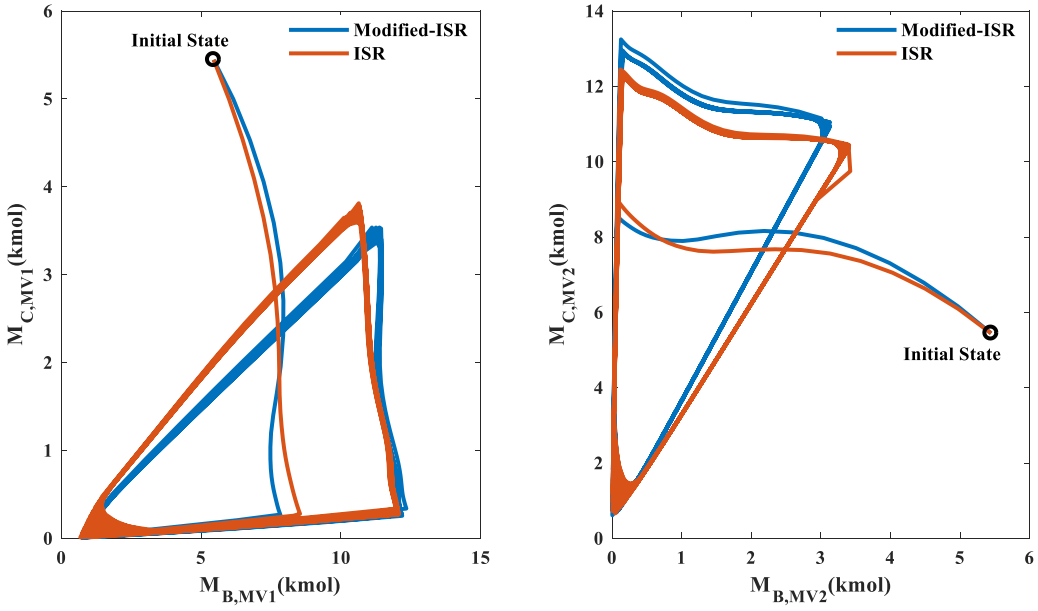

Figure 13 Comparison of the periodic orbits in System V when using the Modified-ISR and ISR control models. MV1 and MV2 refer to the two middle vessels required for separation. $M_{B,MV1}$ and $M_{B,MV2}$ are state variables, which represent the molar holdups of component B in the two middle vessels. Similarly, $M_{c,MV1}$ and $M_{c,MV2}$ are state variables, which represent the molar holdups of component *B* in the two middle vessels

While the results imply that the Modified-ISR control model generates a $S(t)$ that is better in terms of SC when compared to the ISR control model, there is no reason to believe that it is an optimum. Thus, there is the possibility for the existence of an optimum side stream flowrate function $S^*(t)$, which might further reduce the cycle time and in turn minimize SC.

5. Dynamic optimization of semicontinuous distillation systems

Optimizing a semicontinuous distillation system is complex because of periodic processing without start-up or shutdown phases. Historically, Particle Swarm Optimization (PSO) was used to find the best tuning parameter vector, which although had been demonstrated to often find global optima, it cannot be guaranteed. The advantage of using PSO is that the system can be treated as a black-box while the SC is minimized. There is no need for periodic constraints to guarantee that the system returns to starting state of the cycle as it is taken care of by the event-driven tasks in the black-box simulation model. However, one of the disadvantages of the PSO approach is that the time required to find an improved design is large because it generally requires more function evaluations than mathematical programming methods with access to the model equations.

Therefore, to find better trajectories for the side stream flow rate, we used a dynamic optimization approach. The optimization problem was solved using the Aspen Dynamics built-in optimization tool (Aspen Technologies), which uses control vector parametrization or a direct sequential approach (Cervantes and Biegler, 2009). In this method, the control variable (side stream valve

opening) is discretized over the time domain with variable element size and is approximated to be a piecewise linear function. This discretization breaks the problem into two sub-problems; the initial value problem, and the NLP program. The time invariant parameters of the piecewise linear function, element size, the final time, and the tuning parameters values of DB control, at the optimum, were decision variables, which are all determined by DMO, a Successive Quadratic Program (SQP) solver. A DAE solver in the inner loop provides objective function information and gradient information to the NLP solver that is operating in an outer loop (Aspen Technologies). This method could have convergence issues in the case of ill-conditioned systems (Biegler, 2010). Hence, tighter tolerances were chosen to accurately integrate the sensitivity equations. The method used to integrate the DAE system was backward difference formula of maximum order 5, with an absolute and relative tolerance of 0.00005. This is an adaptive step size, multi-step method that is typically used to solve DAE systems of index 1 (Ascher and Petzold, 1998). The initial step size was chosen to be 0.001 with a step reduction factor of 0.5. An initial estimate of the control function is necessary to solve the sequence of quadratic programming sub-problems in the SQP method.

Before running the dynamic optimization, the system is allowed to converge to a stable periodic orbit using the Modified-ISR feedback-PI control of side stream, which is the current best known. Using dynamic optimization, the side stream flow rate trajectory that moves the system away from the Modified-ISR generated periodic orbit to a different periodic orbit with lower SC is found. The design variables that are invariant include the number of trays, the charge volume, reflux drum size, the size of the sump, feed tray location and side draw location. While the optimum is sensitive to all these fixed parameters, the objective of this study is to find an improved $S(t)$ that results in stable cycles with lower SC for a given design configuration. Endpoint constraints that ensure product purities and cycle periodicity are enforced.

The resulting "DO-optimized" side draw flow rate trajectory ($S^*(t)$)—or more appropriately, the resulting side stream valve opening schedule—is then tested by implementation to evaluate its performance and stability over many cycles. This is achieved by re-simulating 10 cycles from the beginning of the separating mode of a stable cycle using the side stream valve opening schedule exactly but allowing the cycle to terminate early when the middle vessel purity conditions have been reached. Or, if the middle vessel purity conditions have not yet been reached at the end of the valve opening schedule, the final valve opening is maintained until the purity conditions have been reached.

5.1 Optimization problem formulation

The objective function to be minimized is the separating cost, which is defined in equation (4),

The optimization problem formulation is,

$$\underset{p_i,\ K_j,\ \tau_j,\ t_f}{\textit{minimize}} \quad \text{SC}$$

$$\textit{subject to} \quad \text{Mass Balance Constraints}$$
$$\text{Energy Balance Constraints}$$
$$\text{Momentum Balance Constraints}$$

Equilibrium Relationships

All other model equations

$$v_{s,i}^{l} \leq v_{s,i} \leq v_{s,i}^{u}, \quad i=1, 2, 3, \ldots N.$$

$$h_{MV}^{l}(t_f) \leq h_{MV}(t_f) \leq h_{MV}^{u}(t_f)$$

$$x_{Di,A}{}^{l} \leq \langle x_{Di,A} \rangle \leq x_{Di,A}{}^{u}$$

$$x_{Bo,C}{}^{l} \leq \langle x_{Bo,B} \rangle \leq x_{Bo,B}{}^{u}$$

$$K_j^{l} \leq K_j \leq K_j^{u}$$

$$\tau_j^{l} \leq \tau_j \leq \tau_j^{u}$$

$$t_f^{l} \leq t_f \leq t_f^{u}$$

where p_i represents the vector of time invariant parameters including the element size in the i^{th} interval and $v_{s,i}$ is the side stream valve opening at the end of the i^{th} interval. All other variables have their usual meanings.

The initial guesses for the side stream valve openings at the end points of each interval were set to corresponding valve openings resulting from the improved Modified-ISR control model found in the previous sections.

5.2 Dynamic Optimization results

The improved valve opening function $v_s(t)$ found using dynamic optimization for the ternary systems compared to using Modified-ISR control model is shown in Figure 14. The system using the results of the dynamic optimization reaches a 100% valve opening faster and moreover, the valve is open more for a slightly longer period during the cycle (Figure 14). Nevertheless, the cycle times are approximately the same as the cycle times when Modified-ISR feedback-PI control was implemented, with a decrease of only 2% at most. Additionally, the convergence of the optimization problem to a solution (for ternary systems) that satisfies the periodic constraint ($h_{MV}^{l}(t_f) \leq h_{MV}(t_f) \leq h_{MV}^{u}(t_f)$) was extremely difficult because of frequent line search and QP sub-problem failures and required manual solver parameter tuning. For the quaternary system (V), the optimizer could not converge to a solution again because of similar numerical issues as stated above although the initial guess was feasible. Solver parameter tuning could not solve the problem.

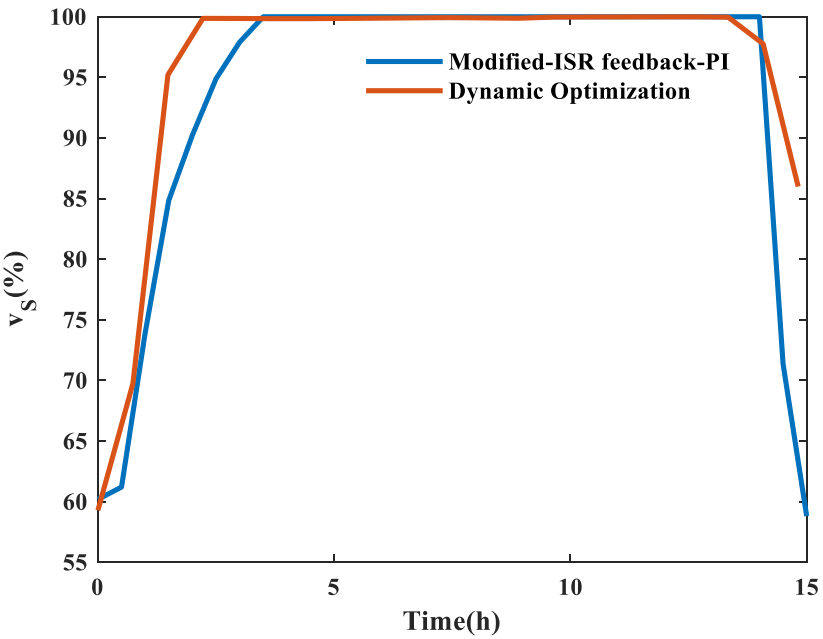

Figure 14 Compares the side stream valve opening percentages in a stable cycle between Modified-ISR feedback-PI control and dynamic optimization (system II).

New semicontinuous cycles were generated through repeated application of this "DO-optimized" control function (Figure 15); moving away from the periodic orbit obtained from using the Modified-ISR feedback-PI control. The trajectory is dense during the end of the charging mode (or the beginning of the separating mode) because the system is not exactly periodic. This is due to the relaxation of periodicity while implementing the periodic constraint in the optimization problem formulation.

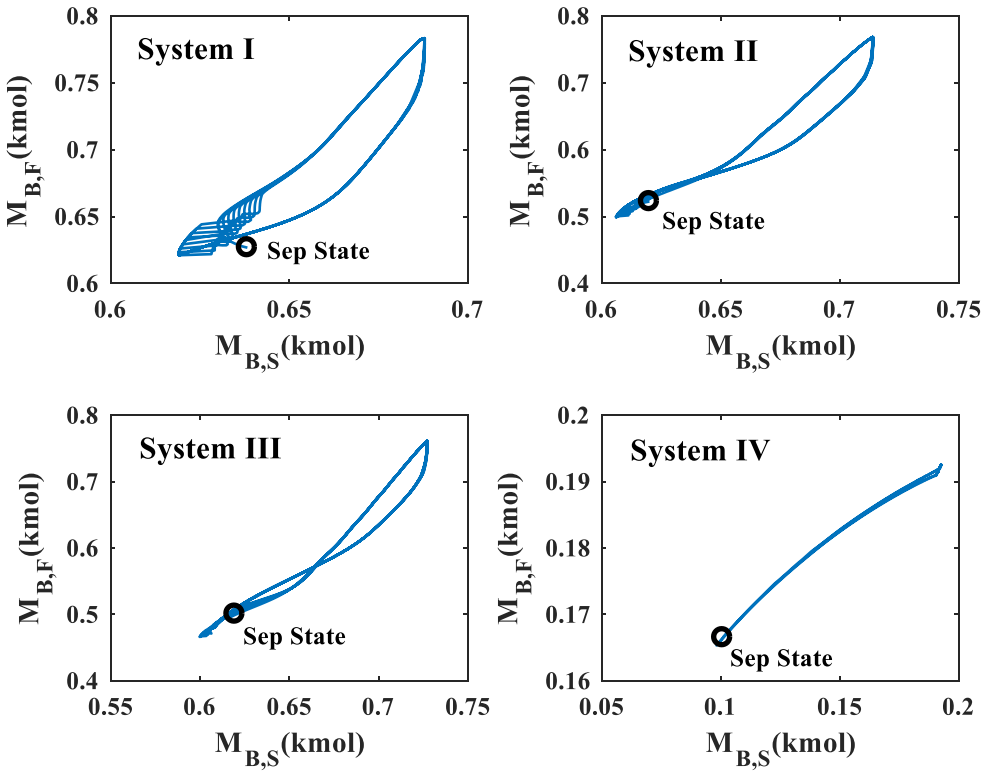

Figure 15 Phase plane plots to illustrate the dynamic behaviour when using the DO-optimized side stream valve opening (control) obtained using dynamic optimization (systems I through IV). Here, "Sep State" refers to the beginning of the Separating (*Sep*) mode of a stable cycle obtained by using the Modified-ISR feedback-PI side stream control and is also the initial state for simulation.

This emphasizes the need to develop an algorithm to find the optimal side stream trajectory that converges the system to a stable cycle from a chosen initial state. Although this is ideal, it is extremely difficult because of the complexity of the system. The SC computed is approximately 1 to 2% lower (see Table 4) when compared to the Modified-ISR case and almost 20% lower when compared to the ISR case. Furthermore, since SQP finds the local optimum, this result, while better than the Modified-ISR case in terms of SC, may not be the global best.

6. Conclusion and Future Work

The present work dealt with the effects of different choices for the side stream flowrate function $S(t)$ on SC, which was studied using simulation experiments on five different systems. The ISR control model was used in almost all prior semicontinuous studies available in the literature. The present study showed that by changing the functional structure of the control model, the periodic orbit in which the system is operated is dramatically different. The newly proposed Modified-ISR control model has not only resulted in stable periodic cycles, but also contributed to lower cycle times and correspondingly lower SC for all five case studies. A lower cycle time increases the frequency at which the feed is processed, thus leading to greater production for the

same capital cost. It was found that by using the Modified-ISR feedback-PI control there was about 10 to 19% reduction in SC when compared to the status quo (ISR feedback-P control). This indicates the importance of a good side draw control for economic semicontinuous distillation design. The presence of better $S(t)$ functions in terms of reducing SC, motivated the search for optimal control functions using dynamic optimization.

Dynamic optimization with periodic constraints of a representative semicontinuous cycle (obtained by using the Modified-ISR feedback-PI control as the initial guess) to find an improved side stream trajectory, $S^*(t)$, that minimizes SC was carried out. While acknowledging that the results may be sub-optimal for other semicontinuous cycles, a trajectory that resulted lower cycle times and lower SC when compared to Modified-ISR feedback-PI control was found. For all practical purposes the improved side stream trajectory obtained through this procedure yielded an addition of one cycle per year (out of hundreds), which is a small improvement. Future work on the value of applying a model predictive control for finding the optimal $S(t)$ during a cycle when compared to Modified-ISR control model is suggested, for constant and varying feed conditions. There is also anecdotal evidence that arose during the study which suggests that the initial state might have some influence on the converged cycle trajectories and will be investigated in the future.

Acknowledgements

Support for this research is made possible through a grant from an Ontario Research Fund—Research Excellence Grant, number ORF-RE 05-072.

Abbreviations

A	Low volatile component
B	Intermediate boiling component
C	High volatile component in ternary mixture / Intermediate boiling component in quaternary mixture
D	High volatile component in quaternary mixture
MV	Middle Vessel
MV1	Middle Vessel to concentrate B in the quaternary separation
MV2	Middle Vessel to concentrate C in the quaternary separation
Ch	Charging Mode
Dis	Discharging Mode
Sep	Separating Mode
spec	Specification
DB	Distillate-Bottom control configuration
P	Proportional controller

PI	Proportional Integral controller
BTX	Benzene, Toluene, and O-Xylene
DME	Dimethyl Ether
MeOH	Methanol
ISR	Ideal Side draw recovery
PV	Process Variable
SP	Setpoint

Nomenclature

$S(t)$	Actual side stream flow rate at a given time (kmol/h)
$S_1(t)$	Actual side stream flow rate at a given time in quaternary system (kmol/h)
$S_2(t)$	Actual side stream flow rate at a given time in quaternary system (kmol/h)
$S_{ISR}(t)$	Side stream flow rate as predicted by the ISR control model (kmol/h)
$S_{ISR,1}(t)$	S_1 as predicted by the ISR control model (kmol/h)
$S_{ISR,2}(t)$	S_2 as predicted by the ISR control model (kmol/h)
$S_{MISR}(t)$	Side stream flow rate as predicted by the Modified-ISR control model (kmol/h)
$S_{MISR,1}(t)$	S_1 as predicted by the Modified-ISR control model (kmol/h)
$S_{MISR,1}(t)$	S_1 as predicted by the Modified-ISR control model (kmol/h)
$S^*(t)$	Improved side stream flow rate as a function of time (kmol/h)
$F(t)$	Feed flow rate to the column as a function of time (kmol/h)
$F_1(t)$	Feed flow rate to the column from MV1(kmol/h)
$F_2(t)$	Feed flow rate to the column from MV2 (kmol/h)
$F_{Dis}(t)$	Middle vessel discharge flow rate (kmol/h)
$F_{MV}(t)$	Flow rate of feed to the middle vessel (kmol/h)
$Di(t)$	Distillate flow rate as a function of time (h)
$Bo(t)$	Bottoms flow rate as function of time (h)
$t_{f,Ch}$	Time at the end of the charging mode (h)
$t_{i,Ch}$	Time at the beginning of the charging mode (h)
$t_{f,Sep}$	Time at the end of the separating mode (h)
$t_{i,Sep}$	Time at the beginning of the separating mode (h)

$t_{f,Dis}$	Time at the end of the discharging mode (h)
$t_{i,Dis}$	Time at the beginning of the discharging mode (h)
t_f^l	Lower bound on the final time (h)
t_f^u	Upper bound on the final time (h)
h_{MV}^u	Upper bound on the height of liquid in the middle vessel (m)
h_{MV}^l	Lower bound on the height of liquid in the middle vessel (m)
$x_{MV,B}(t)$	Mole fraction of component B in the middle vessel at any given time (fraction)
$x_{Di,B}(t)$	Mole fraction of component B in the distillate stream at any given time (fraction)
$x_{Bo,B}(t)$	Mole fraction of component B in the bottom stream at any given time (fraction)
$x_{S,B}(t)$	Mole fraction of component B in the side stream at any given time (fraction)
$x_{MV,B}^{spec}$	Desired specification of component B in the middle vessel (fraction)
$x_{Di,A}(t)$	mole fraction of benzene in the distillate stream (fraction)
$x_{Bo,B}(t)$	mole fraction of benzene in the bottoms stream (fraction)
$\langle x_{Di,A} \rangle$	integral average mole fraction of A in the distillate stream (fraction)
$\langle x_{Bo,B} \rangle$	integral average mole fraction of C in the distillate stream (fraction)
$x_{MV1,B}(t)$	mole fraction of B in MV1 (fraction)
$x_{MV2,B}(t)$	mole fraction of B in MV2 (fraction)
$x_{MV1,C}(t)$	mole fraction of C in MV1 (fraction)
$x_{MV2,C}(t)$	mole fraction of C in MV2 (fraction)
$x_{S_1,B}(t)$	mole fraction of B in S_1 (fraction)
$x_{S_2,B}(t)$	mole fraction of B in S_2 (fraction)
$x_{S_1,C}(t)$	mole fraction of C in S_1 (fraction)
$x_{S_2,C}(t)$	mole fraction of C in S_2 (fraction)
T	Total cycle time (h)
SC	Separation cost ($/kmol)
$v_s(t)$	Side stream valve opening at any given time (%)
$v_{i,s}$	valve opening percentage at the end of the i^{th} discretized element (%)

$v_{i,s}^{l}$	lower bound on the valve opening percentage at the end of the i^{th} discretized element (%)
$v_{i,s}^{u}$	upper bound on the valve opening percentage at the end of the i^{th} discretized element (%)
$\bar{v}_s$	steady state side stream valve opening (%)
K_{Di}	proportional gain of the distillate stream composition controller
K_{Bo}	proportional gain of the bottoms stream composition controller
K_S	proportional gain of the side stream composition controller
K_j^l	lower bound on the proportional gain of the j^{th} controller
K_j^u	upper bound on the proportional gain of the j^{th} controller
τ_{Di}	integral time constant of the distillate stream composition controller (min)
τ_{Bo}	integral time constant of the bottoms stream composition controller (min)
τ_S	integral time constant of the side stream composition controller (min)
τ_j^l	lower bound on the integral time constant of the j^{th} controller (min)
τ_j^u	upper bound on the integral time constant of the j^{th} controller (min)
$\emptyset(t_f)$	Objective function value at the final time
C_r	cost of the refrigerant ($/GJ)
C_s	cost of low pressure saturated steam ($/GJ)
$Q_c(t)$	condenser duty as a function of time (GJ/h)
$Q_r(t)$	reboiler duty as a function of time (GJ/h)

REFRERENCES

Adams II, T.A., Pascall, A., 2012. Semicontinuous Thermal Separation Systems. Chemical Engineering and Technology 35, 1153–1170.

Adams II, T.A., Seider, W.D., 2008. Semicontinuous distillation for ethyl lactate production. AIChE Journal 54, 2539–2552.

Ascher, U.M., Petzold, L.R., 1998. Computer Methods for Ordinary Differential Equations and Differential-Algebraic Equations. Statewide Agricultural Land Use Baseline 2015 1, 332.

Aspen Technologies. Aspen Plus V10.0, AspenTech. http://www.aspentech.com/products/Aspen-Plus/V10/ (accessed 7.31.17).

Ballinger, S.E., Adams, T.A., 2017. Space-constrained purification of dimethyl ether through process intensification using semicontinuous dividing wall columns. Computers and Chemical Engineering 105, 197–211.

Biegler, L.T., 2010. Nonlinear Programming, Society for Industrial and Applied Mathematics. Society for Industrial and Applied Mathematics.

Bristol, E., 1966. On a new measure of interaction for multivariable process control. IEEE Transactions on Automatic Control 11, 133–134.

Cervantes, A., Biegler, L.T., 2009. Optimization Strategies for Dynamic Systems. Encyclopedia of Optimization 2750–2757.

Gupta, B.S., Lee, M.J., 2013. Isobaric vapor-liquid equilibrium for binary systems of toluene+o-xylene, benzene+o-xylene, nonane+benzene and nonane+heptane at 101.3kPa. Fluid Phase Equilibria 352, 86–92.

Gupta, B.S., Lee, M.J., 2012. Isobaric vapor-liquid equilibrium for the binary mixtures of nonane with cyclohexane, toluene, m-xylene, or p-xylene at 101.3kPa. Fluid Phase Equilibria 313, 190–195.

IESO, n.d. Global Adjustment Components and Costs. http://www.ieso.ca/sector-participants/settlements/global-adjustment-components-and-costs (accessed 7.31.17).

Ling, H., Luyben, W.L., 2009. New control structure for divided-wall Columns. Industrial and Engineering Chemistry Research 48, 6034–6049.

Luyben, W.L., 2006. Distillation Design and Control Using ASPEN Simulation, America.

Meidanshahi, V., Adams II, T.A., 2016. Integrated design and control of semicontinuous distillation systems utilizing mixed integer dynamic optimization. Computers and Chemical Engineering 89, 172–183.

Meidanshahi, V., Adams II, T.A., 2015. Chemical Engineering Research and Design A new process for ternary separations : Semicontinuous distillation without a middle vessel. Chemical Engineering Research and Design 93, 100–112.

Meidanshahi, V., Corbett, B., Adams II, T.A., Mhaskar, P., 2017. Subspace model identification and model predictive control based cost analysis of a semicontinuous distillation process. Computers & Chemical Engineering 103, 39–57.

Pascall, A., Adams II, T.A., 2014. Semicontinuous separation of bio-dimethyl ether from a vapor-liquid mixture. Industrial and Engineering Chemistry Research 53, 5081–5102.

Pascall, A., Adams II, T.A., 2013. Semicontinuous separation of dimethyl ether (DME) produced from biomass. The Canadian Journal of Chemical Engineering 91, 1001–1021.

Phimister, J.R., Seider, W.D., 2000a. Semicontinuous, middle-vessel distillation of ternary mixtures. AIChE Journal 46, 1508–1520.

Phimister, J.R., Seider, W.D., 2000b. Distillate−Bottoms Control of Middle-Vessel Distillation Columns. Industrial & Engineering Chemistry Research 39, 1840–1849.

Sinnott, R., Towler, G., 2013. Chemical Engineering Design - Principles, Practice and Economics of Plant and Process Design Second Edition, Chemical Engineering Design.

U.S. Energy Information Administration, 2017. March 2017 Monthly Energy Review, Monthly Energy Review.

Wijesekera, K.N., Adams II, T.A., 2015a. Semicontinuous distillation of quaternary mixtures

using one distillation column and two integrated middle vessels. Industrial and Engineering Chemistry Research 54, 5294–5306.

Wijesekera, K.N., Adams II, T.A., 2015b. Semicontinuous Distillation of Quintenary and N-ary Mixtures. Industrial and Engineering Chemistry Research 54, 12877–12890.